

## New Hybrid Power Filter for Power Quality Improvement in Industrial Network

I. Pecha<sup>1</sup>, J. Tlustý<sup>2</sup>, Z. Müller<sup>2</sup>, and V. Valouch<sup>3</sup>

<sup>1</sup> Elektro, Ltd.  
Bouzov, Czech Republic  
E-mail: [ivo.pecha@seznam.cz](mailto:ivo.pecha@seznam.cz)

<sup>2</sup> Department of Electric Power Engineering  
Faculty of Electrical Engineering, CTU  
Prague, Czech Republic  
E-mail: [tlusty@fel.cvut.cz](mailto:tlusty@fel.cvut.cz)

<sup>3</sup> Institute of Thermomechanics  
Academy of Sciences of the Czech Republic  
Prague, Czech Republic  
E-mail: [valouch@it.cas.cz](mailto:valouch@it.cas.cz)

**Abstract.** The new topology and control strategy of the Hybrid Power Filter (HPF) with a split passive part whose impedance is divided into two individual parts tuned to 50 Hz and 250 Hz is presented.

The topology is very effective to mitigate harmonic currents of a non-linear load, especially for high frequencies. The value of the voltage of fundamental frequency at terminals of an electronic power converter is in the range of several percent of that voltage at the Point of Common Coupling (PCC) at the same time. Additionally, the functionality of this HPF is affected by changes of the grid inductance only negligibly.

The behaviour and properties of the new HPF were compared with those for a usual option of the HPF and for a classic passive compensation by simulation done in the Matlab/Simulink environment. The voltage and current responses and their harmonic spectra were also measured in the real industrial plant Remarkplast, Ltd. under different conditions. The results obtained were in the line with those got by a theoretical analysis done in the frequency domain and confirm the priority of the new HPF above other HPF topologies.

### Key words

Hybrid power filter, topology, control strategy, industrial network, simulation, measurement.

### 1. Introduction

Passive Filters (PFs) for harmonic filtration and reactive power compensation have many disadvantages that restrict their efficiency and reliability. Thus, Active Power Filters

(APFs) represent a perspective solution to improve the power quality in transmission and distribution networks [1], [2]. Nevertheless, the higher price of APFs is the main obstacle of their broad utilization, apart from difficulties if an APF is used in high voltage applications.

A Hybrid Power Filter (HPF) that consists of passive elements (PFs) and an active part (APF) seems to be a proper compromise yielding an effective function as well as reasonable price [3]-[6].

There are many different topologies of HPFs. One of them, with good performance criteria, is characterized by series connection of a passive L-C resonant circuit and an APF itself [7].

The new topology and control strategy of the HPF with a split passive part whose impedance is divided into two individual parts tuned to 50 Hz and 250 Hz is presented.

### 2. Industrial Network and HPF Model

The objectives of the work can be stated as follows: to develop the model of a real industrial network in the Matlab/Simulink environment on the basis of measured real data; to analyze the system for different current classic options of harmonic filtration and reactive power compensation in the frequency as well as time domain; to develop a new HPF topology and control strategy that provide better performance criteria in terms of effectiveness of harmonic mitigation and demand laid on an active part of the HPF.

The measurements of harmonic emission and consumed reactive power were performed in the factory Remarkplast, Ltd., Bohuslavice, Czech Republic where many drives of plastic waste extruders and recycling machines are in operation. This industrial plant had been chosen because of presence of broad portfolio of appliances and non-linear loads producing harmonics and influencing power quality.

Overview of loads in the factory is presented in Tab. 1.

Table I. - Overview of Loads in Factory Remarkplast, Ltd.

Type of load	Total load powers $S_A$ (kVA)	Powers of loads producing harmonics $S_{OS}$ (kVA)
IM connected directly to grid	93	—
IM fed via frequency converters	365	365
DC motors fed from rectifiers	42	42
Heating	52	—
Fluorescent lighting	15	15
Total factory input power	567	422

The basic principle of parallel connection of the new HPH to a non-linear load is shown in Fig. 1. The HPH is characterized by a split passive part whose impedance is divided into two individual parts tuned to 50 Hz and 250 Hz.

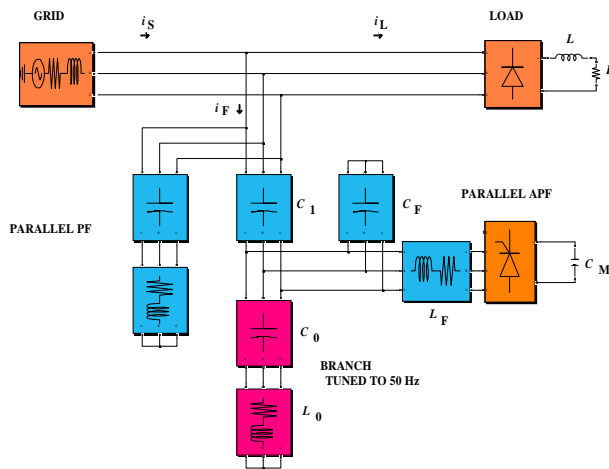


Fig. 1. Scheme of HPH with two individual passive parts tuned to 50 Hz ( $Z_0$ ) and 250 Hz ( $Z_1+Z_0$ ) connected to grid together with classic parallel PF

The basic arrangement of the controller is shown in Fig. 2. Based on the position of the Manual Switch1 we can simulate the function of either the feedback (Switch1 in upper position and  $Gain5 > 1$ ) or feedforward (Switch1 in lower position and  $Gain5 = 1$ ) HPH control. The RMS value of the measured current is calculated, multiplied by a harmonic signal with the grid frequency (produced by PLL circuits) and subtracted from the original current. Thus, the harmonic current, which should be generated by the HPH to compensate harmonic load current, is obtained. The controller is synchronized by two PLL circuits. The first

one (PLL1) generates the synchronization signal determined by the measured current, while the signal of the second PLL2 circuit is deduced from the voltage in the Point of Common Coupling (PCC). If only the signal of the PLL1 is used (Switch2 in lower position), only the load current harmonics are compensated for, otherwise the reactive power compensation is done too.

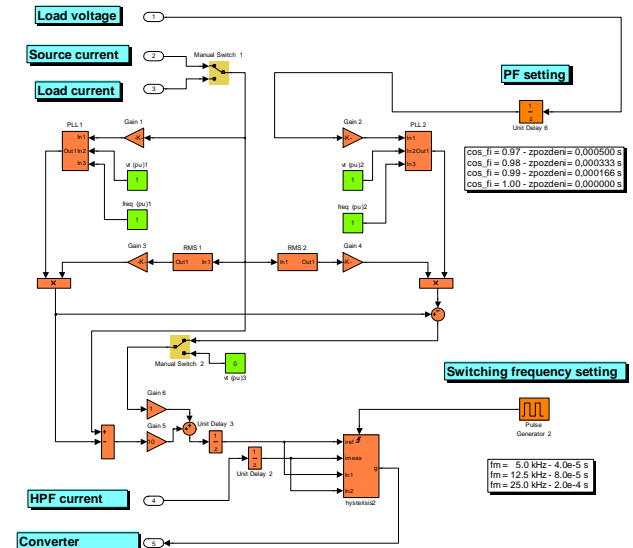


Fig. 2. Structure of HPH controller

The demanded Power Factor of the grid current can be determined by changing the delay of the block Unit Delay6.

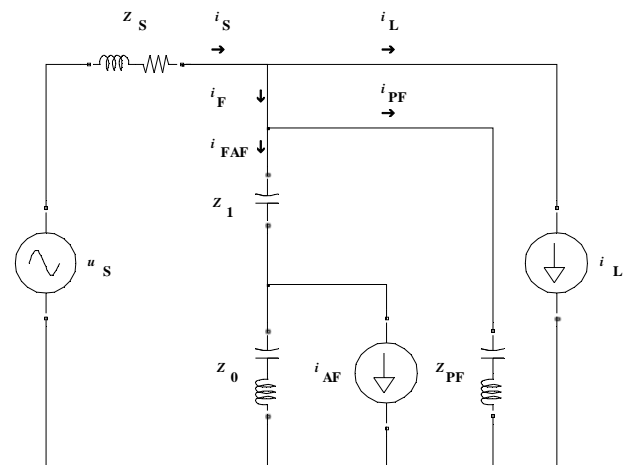


Fig. 3. One phase equivalent scheme of the proposed HPH connected to a non-linear load is shown in Fig. 3.

Equivalent scheme of the proposed HPH is depicted in Fig. 3. On the basis of this circuit we can find the transfer functions as well as frequency characteristics among input variables  $u_s$ ,  $i_L$  and output variables  $i_s$ ,  $u_L$ . The frequency characteristics of simpler topologies may be deduced by a proper choice of the impedances of individual branches of the scheme in Fig. 3. For example, the topology with the series connection of a passive L-C resonant circuit and the APF, mentioned before, may be obtained by setting  $Z_0 \rightarrow \infty$ .

### 3. Result of Simulation and Measurement

The frequency characteristics  $F_{SL} = i_S/i_L$  of the proposed HPF for different gains in the feedback control algorithm ( $K=Gain5$  in Fig. 2) are compared in Fig. 4. The gain  $K=0$  means that only the passive parts are in function.

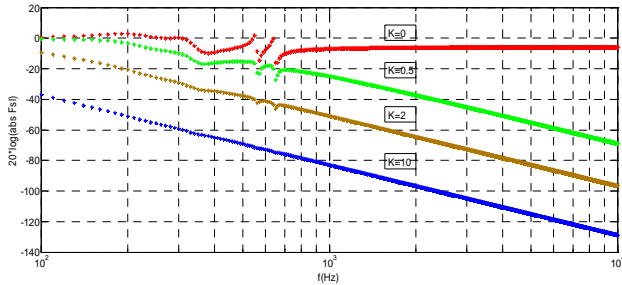


Fig. 4.  $F_{SL} = i_S/i_L$  of the HPF for different gains of the feedback control

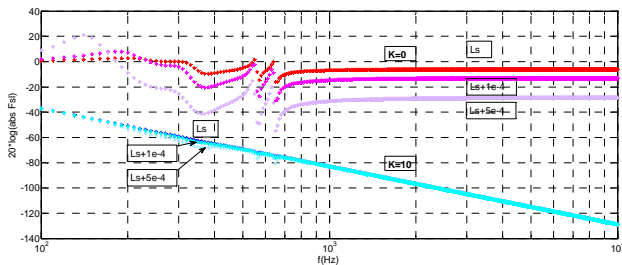


Fig. 5.  $F_{SL} = i_S/i_L$  of the passive parts ( $K=0$ ) and of the HPF ( $K=0$ ) for different values of the grid inductance

Fig. 5 shows how the frequency characteristics  $F_{SL} = i_S/i_L$  are influenced by the changes of the grid inductance. We see that for only passive parts in function the characteristics depend extensively on the grid inductance value, while for the full HPF these changes are insignificant.

Fig. 6 compares the frequency characteristic  $F_{SL} = i_S/i_L$  for the HPF with the series connection of only one passive L-C resonant circuit and the APF ( $Z_0 \rightarrow \infty$ , blue curve) to that for the proposed HPF with the split passive part shown in Fig. 1 (red curve). Both the characteristics are similar up to the frequency of about 600–700 Hz (feedback control,  $K=Gain5=10$ ), but for higher frequencies the proposed HPF (red curve) yields much higher attenuation of the harmonics in the grid current than the known simpler HPF topology.

Fig. 7 compares the frequency characteristics  $F_{AFL} = i_{AF}/i_L$  of the same two HPF options. It is evident that the proposed HPF with the split passive part needs for some value of the harmonic load current  $i_L$  much lower magnitude of the current  $i_{AF}$  generated by the converter of the HPF active part than the topology without  $Z_0$ . According to the previous Fig. 6, the proposed HPF

topology mitigates the harmonic load current, especially above 300 Hz, better than the topology without  $Z_0$ .

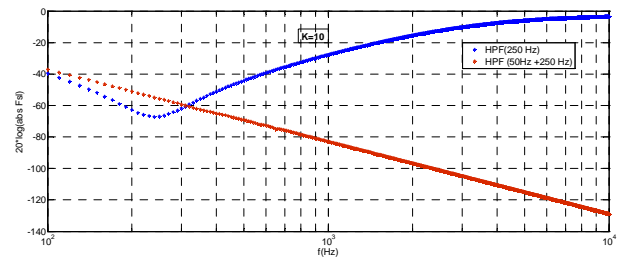


Fig. 6.  $F_{SL} = i_S/i_L$  for the HPF with the series connection of only one passive L-C resonant circuit and the APF ( $Z_0 \rightarrow \infty$ , blue curve) to that for the proposed HPF with the split passive part shown in Fig. 1 (red curve)

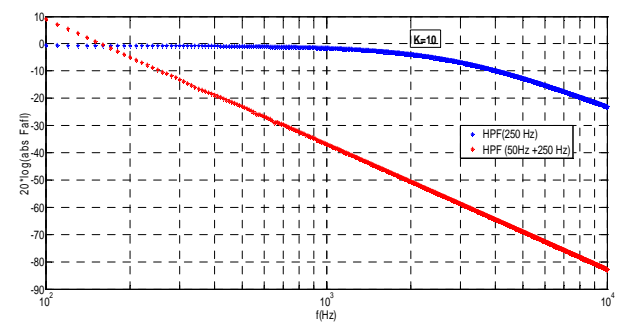


Fig. 7.  $F_{AFL} = i_{AF}/i_L$  for the HPF with the series connection of only one passive L-C resonant circuit and the APF ( $Z_0 \rightarrow \infty$ , blue curve) to that for the proposed HPF with the split passive part shown in Fig. 1 (red curve)

After evaluating the key frequency characteristics of both the compared HPF topology the voltage and current responses and their harmonic spectra were measured in the real industrial plant Remarkplast, Ltd. under different conditions (without compensation, with traditional central passive compensation) and compared to the results obtained by the simulation done in Matlab/Simulink environment for the same conditions. Further, these results were compared to the data obtained when the both HPF topologies were applied.

Fig. 8 shows voltage and current waveforms measured at the input point of the factory without any reactive power compensation (for maximum machine loads).

Fig. 9 shows similar transients if a classical central reactive power compensation with 5, 10, 15, 25 a 60 kVAr steps of condenser batteries controlled by a reactive power controller set to  $PF=0.97$  was applied.  $PF$  without any reactive power compensation reaches  $PF=0.81$ .

Comparing the waveforms in Figs. 8, 9 to those obtained by the simulation of the factory network model under the same conditions we have found that an agreement is good, so we can expect that the model of the network with the HPF models included will provide us also with valid results.

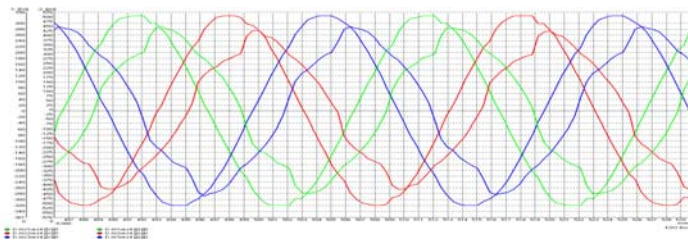


Fig. 8. Voltage and current waveforms measured at the input point of the factory without any reactive power compensation (for maximum machine loads)

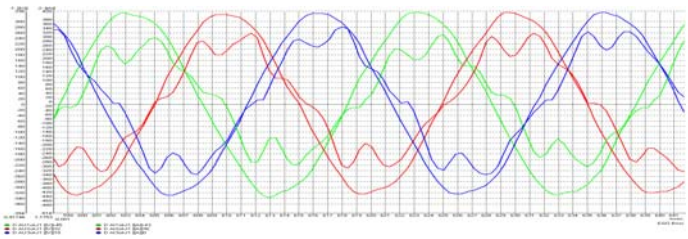


Fig. 9. Voltage and current waveforms measured at the input point of the factory with classical central reactive power compensation with 5, 10, 15, 25 a 60 kVAr steps of condenser batteries

Fig. 10 presents the simulated three phase grid currents when the proposed HPF was used. We see that the current responses are much better than those without (Fig. 8) and with (Fig. 9) classical compensation.

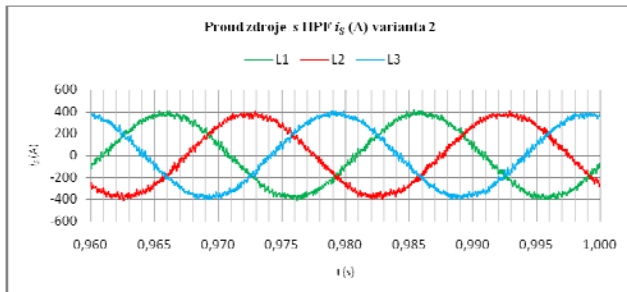


Fig. 10. Simulated three phase grid currents when the proposed HPF was used (full load)

Figs. 11-14 are presented to make it possible to compare both the HPF topologies (without and with the branch with  $Z_0$  impedance) in terms of grid current harmonic spectra and the waveform of the compensating current generated by the electronic power converter (the lower, the better). Again, these figures confirm the priority of the proposed HPF before the classical topology without the branch with  $Z_0$  impedance.

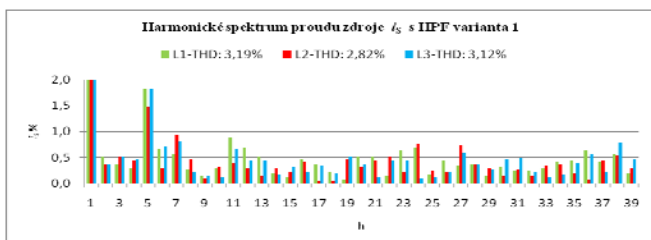


Fig. 11. Grid current  $i_s$  harmonic spectrum for HPF without  $Z_0$  impedance

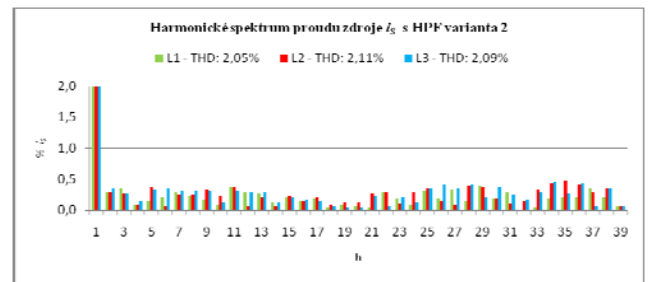


Fig. 12. Grid current  $i_s$  harmonic spectrum for proposed HPF in operation

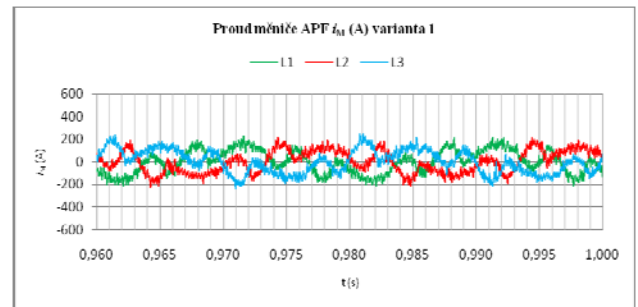


Fig. 13. Electronic power converter current  $i_M$  for HPF without  $Z_0$  impedance

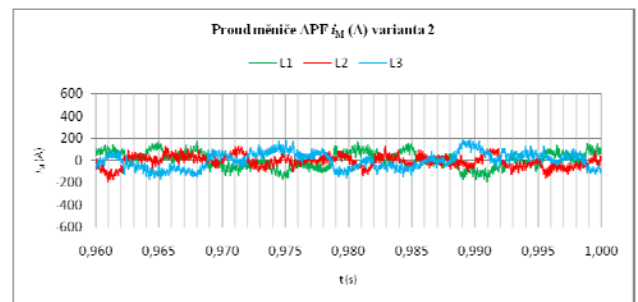


Fig. 14. Electronic power converter current  $i_M$  for proposed HPF in operation

Tab. 2 compares calculated average RMS values of  $U_L$ ,  $I_L$ ,  $I_M$  (converter current), average values of  $P$ ,  $Q$ ,  $S$ , THD, and PF (demanded PF=0.97) for uncompensated industrial plant and for different type of compensation. Comparing  $THD_{US}$ ,  $THD_{IS}$ , and  $I_M$  for both the HPF topologies (without and with the branch with  $Z_0$  impedance) we see quantitative differences between these two topologies.

Table II. - Calculated average RMS values of  $U_L$ ,  $I_L$ ,  $I_M$  average values of  $P$ ,  $Q$ ,  $S$ , THD, and PF (demanded PF=0.97)

Type of compensation	$U_L$ (V)	$I_L$ (A)	$I_M$ (A)	$THD_{US}$ (%)	$THD_{IS}$ (%)	PF (-)
Without compensation	225	304	-	2.56	16.8	0.81
With classical compensation	228	301	-	4.66	28.3	0.97
HPF without $Z_0$	227	301	72.4	0.45	2.09	0.97
Proposed HPF	227	301	35.0	0.38	1.45	0.97

Generally, we can come to the conclusion that the proposed HPF topology with split passive part effectively compensates for the load current harmonics with low harmonic currents generated by the converter of the active part of the HPF, while the higher the frequency is,

the more effective the HPF operation becomes. At the same time, the voltage of the fundamental frequency at the converter terminals is only at the level of several percent of the voltage at the PCC.

#### 4. Conclusion

The new topology and control strategy of the HPF with a split passive part whose impedance is divided into two individual parts tuned to 50 Hz and 250 Hz is presented.

The behaviour and properties of the new HPF were compared with those for a usual option of the HPF and for a classic passive compensation by simulation done in the Matlab/Simulink environment. The results obtained were in the line with those got by a theoretical analysis done in the frequency domain and confirm the priority of the new HPF above other HPF topologies.

The voltage and current responses and their harmonic spectra were also measured in the real industrial plant Remarkplast, Ltd. under different conditions (without compensation, with classical central reactive power compensation) with good agreement with results of the simulation of the factory network model under the same conditions.

The topology is very effective to mitigate harmonic currents of a non-linear load, especially for high frequencies. The value of the voltage of fundamental frequency at terminals of an electronic power converter is in the range of several percent of that voltage at the PCC at the same time.

#### Acknowledgement

The financial support of the Grant Agency of the Academy of Sciences of the Czech Republic (project no. IAA200760703), Institutional Research Plan Z20570509 of the Institute of Thermomechanics of the ASCR, v.v.i., and of the Ministry of Education, Youth, and Sports (Research Plan MSM 6840770017 of the Czech Technical University) are highly acknowledged.

#### References

- [1] L. Gyugyi, E.C. Strycula, Active ac power filters, Proc. IEEE/ Ind. App. Soc. Annu. Meeting, 1976, pp. 529-535.
- [2] N. Mohan, H.A. Peterson, W.F. Long, G.R. Dreifuerst, J.J. Vithayathil, Active filters for AC harmonic suppression, IEEE Power Eng. Soc. Winter Meeting, 1977, paper A77026-8.
- [3] F. Peng, H. Akagi, A. Nabae, A new approach to harmonic compensation in power system-A combined system of shunt passive and series active filters, IEEE Trans. Ind. Appl., vol. 26, no. 6, Nov./Dec. 1990, pp. 983-990.
- [4] H. Fujita, H. Akagi, The unified power quality conditioner of series and shunt-active filters, IEEE Trans. Power Electron., vol. 13, no. 2, Mar. 1998, pp. 315-322.
- [5] F.Z. Peng, Harmonic Sources and Filtering Approaches, IEEE IA Mag.7, 2001, No.4, pp. 18-25.
- [6] J. Škramlík, V. Valouch, Control Strategy of Hybrid Power Filter, the 8<sup>th</sup> Symposium at Humboldt University, Hannover, Germany, September 27-28, 2006, pp.61-65.
- [7] Q. Chen, Z. Chen, M. McCotnick, The application and optimization of C-type filter in a combined harmonic power filter, the 35th Annu. IEEE Power Electronics Specialists Conf., Aachen, Germany, 2004.
- [8] Z. Shuai, An Luo, Wenji Zhu, Ruixiang Fan, Ke Zhou, Study on a Novel Hybrid Active Power Filter Applied to a High-Voltage Grid, IEEE Trans. on PD, Vol. 24, No. 4, Oct. 2009, pp 2344-2352.

#### Appendix

Parameters of HPH and PFs

Grid	PF1	PF5	PF7	PF11	PF13
$R_S = 0.0113 \Omega$	$R_{PF1} = R = 0.364 \Omega$	$C_{PF5} = 1/(1/C_0+1/C_1)$	$R_{PF7} = 0.02 \Omega$	$R_{PF11} = 0.17 \Omega$	$R_{PF13} = 0.17 \Omega$
$L_S = 0.0493 \text{ mH}$	$L_{PF1} = L_0 = 0.456 \text{ mH}$	$C_1 = 1 \mu\text{F}$	$L_{PF7} = 0.405 \text{ mH}$	$L_{PF11} = 2 \text{ mH}$	$L_{PF13} = 2 \text{ mH}$
	$C_{PF1} = C_0 = 22.22 \mu\text{F}$		$C_{PF7} = 0.51 \mu\text{F}$	$C_{PF11} = 40 \mu\text{F}$	$C_{PF13} = 30 \mu\text{F}$